

High-Field Pauli-Limiting Behavior and Strongly Enhanced Upper Critical Magnetic Fields near the Transition Temperature of an Arsenic-Deficient $\text{LaO}_{0.9}\text{F}_{0.1}\text{FeAs}_{1-\delta}$ Superconductor

G. Fuchs, S.-L. Drechsler,* N. Kozlova, G. Behr, A. Köhler, J. Werner, K. Nenkov, R. Klingeler, J. Hamann-Borrero, C. Hess, A. Kondrat, M. Grobosch, A. Narduzzo, M. Knupfer, J. Freudenberger, B. Büchner, and L. Schultz

IFW Dresden, P.O. Box 270116, D-01171 Dresden, Germany

(Received 4 June 2008; published 4 December 2008; publisher error corrected 5 December 2008)

We report upper critical field $B_{c2}(T)$ data for disordered (arsenic-deficient) $\text{LaO}_{0.9}\text{F}_{0.1}\text{FeAs}_{1-\delta}$ in a wide temperature and magnetic field range up to 47 T. Because of the large linear slope of $B_{c2} \approx -5.4$ to -6.6 T/K near $T_c \approx 28.5$ K, the T dependence of the in-plane $B_{c2}(T)$ shows a flattening near 23 K above 30 T which points to Pauli-limited behavior with $B_{c2}(0) \approx 63$ –68 T. Our results are discussed in terms of disorder effects within conventional and unconventional superconducting pairings.

DOI: 10.1103/PhysRevLett.101.237003

PACS numbers: 74.62.-c, 74.20.Rp, 74.25.Bt, 74.25.Op

The recent discovery of relative high transition temperatures T_c in $\text{LaO}_{0.9}\text{F}_{0.1}\text{FeAs}_{1-\delta}$ [1] has established a new family of superconductors. Since the usual e -ph mechanism has been ruled out by a much too weak coupling strength $\lambda \leq 0.2$ [2], a variety of nonstandard mechanisms mostly involving spin fluctuations have been proposed [3–5]. Naturally, our knowledge about these fascinating systems is still poor at present. Together with the controversially discussed unconventional (p - or d -wave) vs conventional (extended s -wave) symmetry, the magnitude of the superconducting order parameter Δ (gap)[6,7], the upper critical field $B_{c2}(T)$, and its slope near T_c are fundamental quantities characterizing the superconducting state. Because of the involved Fermi velocities v_f in the clean limit, it provides insight into the underlying electronic structure which might be affected by a complex interplay of correlation effects [8,9] and the vicinity of competing magnetism [10–12]. Controlled disorder provides insight into relevant scattering processes and in the symmetry of the pairing, since any unconventional pairing in the sense of T_c and $dB_{c2}/dT|_{T_c}$ is expected to be suppressed by strong disorder [13–16]:

$$-\ln\left(\frac{T_c}{T_{c0}}\right) = \psi\left(\frac{1}{2} + \frac{\beta T_{c0}}{2\pi T_c}\right) - \psi\left(\frac{1}{2}\right), \quad (1)$$

where $\psi(x)$ is the digamma function and β is the strong-coupling pair-breaking parameter $\beta = \Omega_p^2 \rho_0 / 8\pi(1 + \lambda)T_{c0}$, which is related to the residual resistivity ρ_0 and the plasma energy Ω_p in the (a, b) plane. Some, but much weaker, suppression might occur also in the anisotropic or multiband s -wave case since the scattering may smear out the gap anisotropy. However, it will be shown that surprisingly nothing similar happens in our case.

For low applied fields, rather different slopes $dB_{c2}/dT \approx -1.6$ T/K up to -2 T/K at $T_c \approx 26$ K [17,18] and up to -4 T/K at $T_c \approx 20$ K [19] have been reported for the As-stoichiometric La-based compounds. Here we report with $dB_{c2}/dT \approx -5.4$ to -6.6 T/K, to our knowledge one of the highest slopes of B_{c2} near T_c ob-

served so far for the La series. Another interesting issue of high-field studies considered here is the possibility of Pauli-limiting (PL) behavior. Triplet p -wave pairing or strong coupling [$B_{c2}(0) \leq 50$ T] would naturally explain the reported absence of PL behavior [17]. In this context it is important that we succeeded to detect PL behavior for our specific sample. It points to $B_{c2}(0)$ values being much below often-used WHH (Werthamer-Helfand-Hohenberg) [20]-based estimates. After presenting various data which deviate from those of Ref. [17] as well as from our non-deficient As samples [21–25], we will discuss our $B_{c2}(T)$ results in light of these more general issues.

A polycrystalline sample of $\text{LaO}_{0.9}\text{F}_{0.1}\text{FeAs}_{1-\delta}$ was prepared as described in our previous work [21–25] and, e.g., in Ref. [26]. However, in contrast to that work, here a Ta foil was used to wrap the pellets. Ta acts as an As getter at high T forming a solid solution of about 9.5 at. % As in Ta with a small layer of Ta_2As and TaAs on top of the foil. This leads to an As loss in the pellets. The annealed pellets were ground and polished, and the local composition of the resulting samples was investigated by wavelength-dispersive x-ray spectroscopy in a scanning electron microscope. The sample consists of 1–20 μm -sized grains of $\text{LaO}_{0.9}\text{F}_{0.1}\text{FeAs}_{1-\delta}$ ($\delta \sim 0.05$ –0.1) where the F content slightly fluctuates between different grains. A powder x-ray diffraction study with a Rietveld refinement of the main phase yields slightly enhanced lattice constants: $a = 4.02819$ Å and $c = 8.72397$ Å compared to $a = 4.02043(4.02451)$ Å and $c = 8.69552(8.70995)$ Å for our cleanest sample with $T_c = 26.8$ K and an ordinary sample with $T_c = 26$ K, respectively [25]. The latter are almost As-stoichiometric samples with the same $\text{F}_{0.1}$ content. Surprisingly, the lattice constants of the ADS (As-deficient sample) are close to those for underdoped samples near the border of magnetism and superconductivity in stoichiometric samples. The reduced charge of the anionic As layers suggests less attraction between them and the adjacent “cationic” central Fe and the charge reservoir $\text{LaO}_{0.9}\text{F}_{0.1}$ layers. This might explain the increase

of c and due to the weakened Madelung potential also a reduced doping of the Fe layer.

The electrical resistance was measured for a platelike $\text{LaO}_{0.9}\text{F}_{0.1}\text{FeAs}_{1-\delta}$ ADS with nominal dimensions $3 \times 2.6 \times 0.53 \text{ mm}^3$ using the standard four-point method. Its resistivity $\rho(T)$ is shown in Fig. 1. The resistivity of this ADS in the normal state at 30 K, with about $0.6 \text{ m}\Omega \text{ cm}$, clearly exceeds that reported for other $\text{LaO}_{0.9}\text{F}_{0.1}\text{FeAs}$ samples. Nevertheless, our ADS was found to exhibit a rather high T_c value of 28.5 K defined at 90% of ρ in the normal state and a relatively sharp transition width (see inset of Fig. 1) which excludes an anomalous inhomogeneity. The low- T region above T_c with $\rho \propto T^2$, ascribed to a pronounced e - e scattering regarded as evidence for a standard Fermi liquid picture [18], has been somewhat narrowed from 225 to $T \leq 175 \text{ K}$ for this ADS [27]. The $\rho(T)$ dependence of this ADS resembles that of underdoped stoichiometric samples in the range of 0.05–0.07 F content [25]. Since each As site is surrounded by four Fe sites, the effect of even a few As vacancies might be drastic. Thus, a substantial shortening of the mean free path l up to a few lattice constants a as estimated below from the observed enhanced field slope at T_c seems to be quite reasonable.

In Fig. 2, the electrical resistance of the studied ADS is plotted vs T for applied dc fields up to 14 T. Resistance data vs applied field of this ADS measured in pulsed fields up to 50 T are plotted in Fig. 3. Gold contacts (100 nm thick) were made by sputtering in order to provide a low contact resistivity and therefore to avoid possible heating effects in the high-field measurements performed in the 50 T magnet of the Dresden High Magnetic Field Laboratory [28]. The

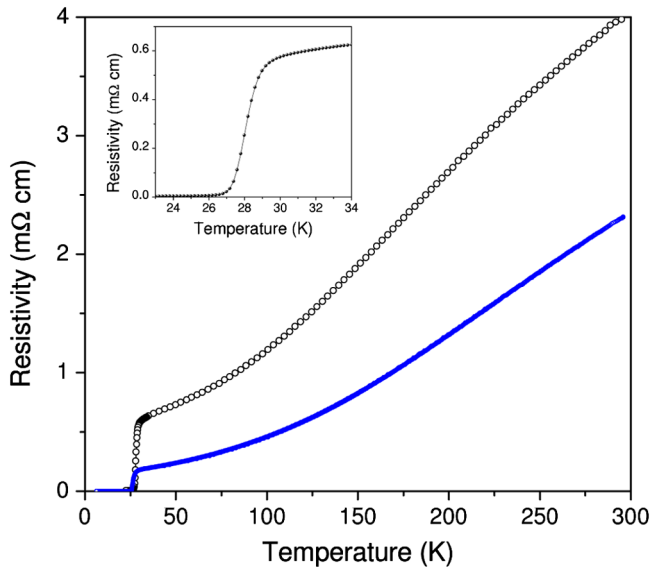


FIG. 1 (color online). Resistivity at zero magnetic field of the $\text{LaO}_{0.9}\text{F}_{0.1}\text{FeAs}_{1-\delta}$, $\delta \approx 0.05$ – 0.1 ADS studied in the present Letter. The inset shows the resistivity near T_c . Solid line: A cleaner almost stoichiometric sample [25].

agreement between measurements up to 29 and 47 T confirms that our data are not affected by sample heating. At high fields a substantial broadening of the transition curves is observed as shown in both figures. It stems from the large anisotropy of $B_{c2}(T)$ expected for layered compounds as here [4,12]. B_{c2} was determined as in Ref. [17] from the onset of superconductivity defining it at 90% of R_N , the resistance in the normal state. Within a second approach, the magnetoresistance in the normal state was taken into account, and $R_N(T)$ has been described as explained in [27]. For this modified definition of B_{c2} , one gets somewhat higher B_{c2} values and also higher slopes near T_c .

Generally, the B_{c2} values from $0.9R_N$ data refer to those grains which are oriented with their ab planes along the applied field. The $B_{c2}^{ab}(T)$ curve of our ADS is shown in Fig. 4. The comparison of the data from dc and pulsed field measurements in the field range up to 14 T confirms that both data sets do well agree. The $B_{c2}(T)$ curve in Fig. 4 shows a surprisingly steep $dB_{c2}/dT|_{T_c} = -5.4 \text{ T/K}$ (-6.6 T/K within the second approach described above) which exceeds the slopes reported for cleaner non-ADS samples by more than a factor of 2 [17,18,26]. This points to strong impurity scattering in our ADS in accord with its enhanced resistivity at 30 K. For applied fields up to about 30 T, the $B_{c2}(T)$ data can be well described by the standard WHH model [20]. Using $dB_{c2}/dT = -5.4 \text{ T/K}$ (-6.6 T/K) and $T_c = 28.5 \text{ K}$ (28.8 K), this model predicts $B_{c2}^*(0) = -0.69T_c(dB_{c2}/dT)_{T_c} = 106 \text{ T}$ (131 T) at $T = 0$. However, for applied fields above 30 T or below 23 K, increasing deviations of the $B_{c2}(T)$ data from the WHH curve are clearly visible. They increase with applied field. Notice that the resulting difference between the measured $B_{c2}(T)$ and B_{c2}^* is comparable for both definitions of the upper critical field (Fig. 5). The flattening of $B_{c2}(T)$ at high fields points to its limitation by the Pauli spin paramagnetism. This effect is measured in the WHH model by the

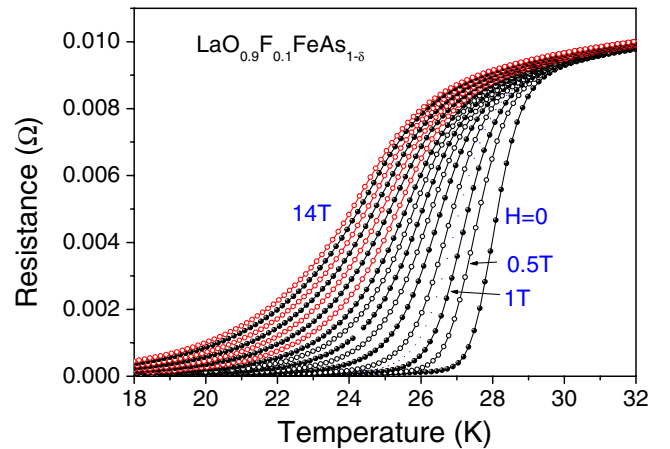


FIG. 2 (color online). T dependence of the resistance R for the ADS for various dc fields up to 14 T. Between 1 and 14 T, the applied magnetic field was increased in steps of 1 T.

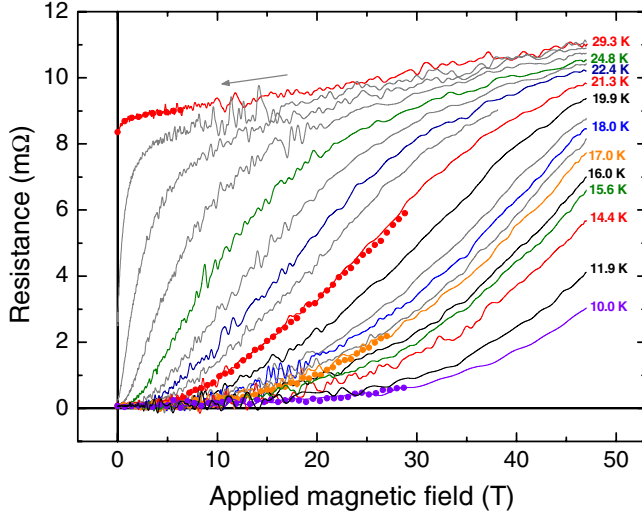


FIG. 3 (color online). Field dependence of the resistance at fixed T (see legend) measured in pulsed fields. Lines: Measurements up to 47 T; symbols: measurements shown for four selected T values.

Maki parameter α :

$$\alpha = \sqrt{2}B_{c2}^*(0)/B_p(0), \quad (2)$$

where $B_p(0)$ is the paramagnetically limited field [29]:

$$B_p(0)[\text{Tesla}] = 1.86\eta_{\text{eff}}(\lambda)T_c[\text{K}], \quad (3)$$

where $\eta_{\text{eff}} = (1 + \lambda)^e \eta_{\Delta} \eta_{B_{c2}} (1 - I)$ is a correction to BCS due to the e boson and e - e interaction [$I = N(0)V$

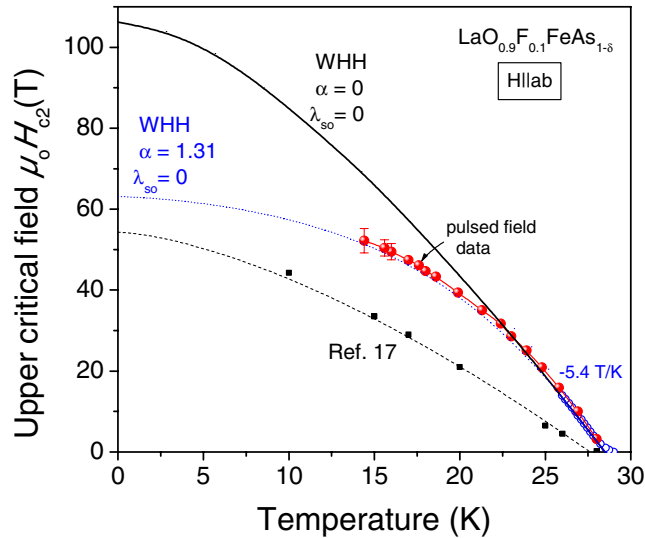


FIG. 4 (color online). B_{c2}^{ab} vs T . Data from dc (\circ) and pulsed field measurements (\bullet). The last three “data points” above 47 T are obtained from Fig. 3 by a linear extrapolation of $R(B) < 0.9R_N$ to $R(B) = 0.9R_N$. Dashed line: Data from Ref. [17]; solid line: WHH model without PL. Dotted line: $B_{c2}^*(T)$ for $\alpha = 1.31$ without spin-orbit scattering.

is the Stoner factor] [29,30]. η_{eff} depends on the e -boson coupling constant λ and $\varepsilon = 0.5, 1$ according to Refs. [29,30], respectively. Because of PL, $B_{c2}(0)$ is lowered:

$$B_{c2}^p(0) = B_{c2}^*(0)/\sqrt{1 + \alpha^2}. \quad (4)$$

Ignoring weak spin-orbit scattering for the sake of simplicity, we get $\alpha = 1.31$ and $B_{c2}^p(0) = 63$ T (68 T) from Eqs. (2)–(4), using $\lambda = 0.5$ [23] for a representative value of the e -boson coupling constant for $\text{LaO}_{0.9}\text{F}_{0.1}\text{FeAs}_{1-\delta}$, $\eta_{\text{eff}} = 2.09$, and $B_{c2}^*(0) = 106$ T (131 T) without PL. The $B_{c2}^p(T)$ line plotted in Fig. 4 is based on Eq. (4) and was obtained by replacing $B_{c2}^*(0)$ entering its numerator and α by $B_{c2}^*(T)$, $\alpha = 0$ of the WHH model. This rough approximation of $B_{c2}^p(T)$ has been used to illustrate the PL in the studied ADS.

High $B_{c2}(0)$ values and similarly for $dB_{c2}/dT|_{T_c}$ can be achieved by: (i) strong coupling, (ii) small Fermi velocities v_f , and (iii) strong intraband scattering. Strong coupling can be excluded empirically for related systems [6,23]. Note that unconventional triplet p - or d -wave pairing [13–15] and (iii) cannot be reconciled. Hence, singlet extended s -wave pairing remains as a reasonable scenario. As mentioned above, the residual resistivity ρ_0 of our ADS is enhanced compared to that of clean samples (Fig. 1) examined so far in our studies. This points to strong intraband scattering. Adopting in accord with the single isotropic gap found for $\text{SmO}_{0.85}\text{F}_{0.15}\text{FeAs}$ [6] an effective single-band s -wave picture [31], $B_{c2}^c(0)$ [and similarly for $B_{c2}^{ab}(0)$], written in convenient units, ignoring PL reads in the clean (cl) and general case:

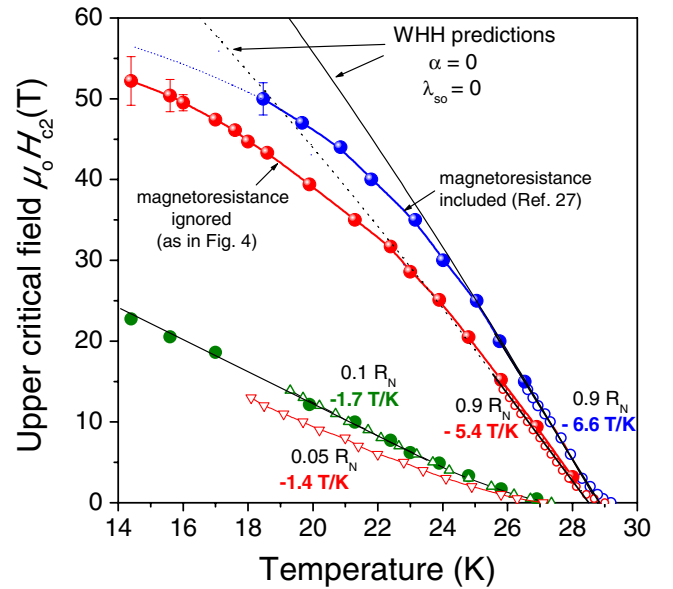


FIG. 5 (color online). Upper critical field vs T from 90%, 10%, and 5% of the normal state resistance R_N . Open (solid) symbols: dc field data—Fig. 2 (pulsed field data—Fig. 3).

$$B_{c_2,cl}^c(0)[T] = 0.0237(1 + \lambda)^{2.2} T_c^2 [K] / v_f^2 [10^5 \text{ m/s}], \quad (5)$$

$$B_{c_2}^c(0) = B_{c_2,cl}^c(0) \{1 + 0.13 \gamma_{\text{imp}} [K] / [T_c(1 + \lambda)]\}, \quad (6)$$

where λ is the relevant e -boson coupling constant, γ_{imp} is the scattering rate, and v_f denotes the in-plane averaged Fermi velocity. The mass anisotropy $\gamma^2 = M/m$ which affects $B_{c_2}^{ab}$ varies according to the local-density approximation predictions [4,12,23] between 6.2 and 15. From the 5% level of the resistivity transition curves (see Fig. 5), a lower limit of about 3.7 for $\gamma = B_{c_2}^{ab}/B_{c_2}^c$ is estimated close to $\gamma \approx 4.5$ for the first single crystal of the whole class (NdO_{0.82}F_{0.12}FeAs [32]). The reduced γ of these samples compared with Refs. [7,33] might be ascribed also to disorder, provided in both cases a less anisotropic Fermi surface sheet is involved like in MgB₂ [34]. The $B_{c_2}(T)$ data for the 10% R_N criterion show no PL up to 33 T. Hence, for $B_{c_2}^c$ no PL is expected. To simulate the substantially enhanced dB_{c_2}/dT at T_c which, estimated in the weak-coupling regime, is $\propto B_{c_2}(0)$ [35], we adopt using Eq. (6) $\gamma_{\text{imp}} \approx 50$ meV, i.e., a situation intermediate between the clean and dirty limits. The ratio between the BCS-coherence length ξ_0 and the mean free path l would be 3.6, justifying roughly the above use of the dirty limit theory valid for $\xi_0/l \gg 1$. The increase of T_c is difficult to understand within a simple s -wave scenario. For instance, in V₃Si, Nb₃Sn, and MgB₂, the slopes of B_{c_2} raise with increasing disorder measured by ρ_0 , whereas their T_c 's slightly decrease [29,34]. Here the raise of T_c might result from (i) an enhanced density of states $N(0)$ due to disorder, if the Fermi energy is located in a tail of a broadened peak of $N(E)$, (ii) spin fluctuation s -wave pairing supported by weak e -ph interaction being pair-breaking in p and d channels, and/or (iii) suppression of competing (local) antiferromagnetism by a reduction of the nesting. If the pairing in the clean samples is indeed unconventional, "nonmonotonic" disorder dependencies should first cause a weakening of that pairing followed by an improved s -wave pairing as probably observed here.

In summary, we reported a high-field study of a LaO_{0.9}F_{0.1}FeAs_{1- δ} sample with improved superconductivity. It exhibits a rather high slope $dB_{c_2}/dT|_{T_c} \approx -5.4$ T/K to -6.6 T/K depending on the used definition of $B_{c_2}(T)$. In all cases at lower T a flattening of the $B_{c_2}(T)$ curve points to PL behavior with $B_{c_2}(0) \approx 63$ –68 T extrapolated. We ascribe this behavior to disorder effects in an extended s -wave state. Thus, controlled disorder provides a useful tool to study the pairing symmetry of these novel superconductors. In view of the achieved improved $dB_{c_2}/dT|_{T_c}$ at a higher T_c value, the introduction of As vacancies or of other defects opens new routes for optimizing their properties. Its study should provide also a deeper insight into the specific role of As $4p$ orbitals played in the formation of quasiparticles relevant for the physical prop-

erties including the magnetic excitations. The PL found here suggests to continue measurements at least up to 70 T in order to elucidate whether there is still much room for increasing B_{c_2} beyond that range. Apparently, the solution of this problem will affect the evaluation of future high-field applications.

We thank M. Deutschmann, R. Müller, S. Pichl, R. Schönfelder, and S. Müller-Litvanyi for technical assistance. Discussions with H. Eschrig, A. Gurevich, I. Mazin, and K. Koepf are gratefully acknowledged.

*Corresponding author.

drechsler@ifw-dresden.de

- [1] Y. Kamihara *et al.*, J. Am. Chem. Soc. **130**, 3296 (2008).
- [2] L. Boeri *et al.*, Phys. Rev. Lett. **101**, 026403 (2008).
- [3] G. Xu *et al.*, arXiv:0803.1282.
- [4] I. I. Mazin *et al.*, Phys. Rev. Lett. **101**, 057003 (2008).
- [5] M. M. Korshunov and I. Eremin, Phys. Rev. B **78**, 140509 (R) (2008).
- [6] T. Y. Chen *et al.*, Nature (London) **453**, 1224 (2008).
- [7] A. Dubroka *et al.*, Phys. Rev. Lett. **101**, 097011 (2008).
- [8] K. Haule *et al.*, Phys. Rev. Lett. **100**, 226402 (2008).
- [9] K. Haule and G. Kotliar, arXiv:0805.0722.
- [10] J. Dong *et al.*, Europhys. Lett. **83**, 27006 (2008).
- [11] Z.-Y. Weng, arXiv:0804.3228.
- [12] D. Singh *et al.*, Phys. Rev. Lett. **100**, 237003 (2008).
- [13] J.-Y. Lin *et al.*, Phys. Rev. B **59**, 6047 (1999).
- [14] C. Petrovic *et al.*, Phys. Rev. B **66**, 054534 (2002).
- [15] A. P. Mackenzie *et al.*, Phys. Rev. Lett. **80**, 161 (1998).
- [16] R. J. Radtke *et al.*, Phys. Rev. B **48**, 653 (1993).
- [17] F. Hunte *et al.*, Nature (London) **453**, 903 (2008).
- [18] A. Sefat *et al.*, Phys. Rev. B **77**, 174503 (2008).
- [19] G. F. Chen *et al.*, Phys. Rev. Lett. **100**, 247002 (2008).
- [20] N. R. Werthamer *et al.*, Phys. Rev. **147**, 295 (1966).
- [21] H. Luetkens *et al.*, Phys. Rev. Lett. **101**, 097009 (2008).
- [22] H.-H. Klauss *et al.*, Phys. Rev. Lett. **101**, 077005 (2008).
- [23] S.-L. Drechsler *et al.*, arXiv:0805.1321 [Phys. Rev. Lett. (to be published)].
- [24] H.-J. Grafe *et al.*, Phys. Rev. Lett. **101**, 047003 (2008).
- [25] C. Hess *et al.* (to be published).
- [26] X. Zhu *et al.*, Supercond. Sci. Technol. **21**, 105001 (2008).
- [27] Within another approach, especially to have an alternative determination of B_{c_2} , where the magnetoresistance was taken into account, the resistance in the normal state $R_N(T)$ has been fitted between T_c and 80 K resulting in $R_N(T) = 7.74 + 1.7 \times 10^{-2} T^{1.4}$ given in m Ω and T in K.
- [28] H. Krug *et al.*, Physica (Amsterdam) **294B–295B**, 605 (2001).
- [29] T. P. Orlando *et al.*, Phys. Rev. B **19**, 4545 (1979).
- [30] M. Schossmann and J. P. Carbotte, Phys. Rev. B **39**, 4210 (1989).
- [31] S. V. Shulga *et al.*, J. Low Temp. Phys. **129**, 93 (2002).
- [32] Y. Jia *et al.*, Appl. Phys. Lett. **93**, 032503 (2008).
- [33] S. Weyeneth *et al.*, arXiv:0806.1024.
- [34] A. Gurevich, Physica (Amsterdam) **456C**, 160 (2007).
- [35] L. N. Bulaevskii *et al.*, Phys. Rev. B **38**, 11290 (1988).